Quantum Monte Carlo calculations of the energetics of small molecules

Michael Hutcheon

Cavendish Laboratory, Department of Physics, J J Thomson Avenue, Cambridge. CB3 0HE

Abstract

Fusce mauris. Vestibulum luctus nibh at lectus. Sed bibendum, nulla a faucibus semper, leo velit ultricies tellus, ac venenatis arcu wisi vel nisl. Vestibulum diam. Aliquam pellentesque, augue quis sagittis posuere, turpis lacus congue quam, in hendrerit risus eros eget felis. Maecenas eget erat in sapien mattis porttitor. Vestibulum porttitor. Nulla facilisi. Sed a turpis eu lacus commodo facilisis. Morbi fringilla, wisi in dignissim interdum, justo lectus sagittis dui, et vehicula libero dui cursus dui. Mauris tempor ligula sed lacus. Duis cursus enim ut augue. Cras ac magna. Cras nulla. Nulla egestas. Curabitur a leo. Quisque egestas wisi eget nunc. Nam feugiat lacus vel est. Curabitur consectetuer.

Contents

1. Introduction

Fusce mauris. Vestibulum luctus nibh at lectus. Sed bibendum, nulla a faucibus semper, leo velit ultricies tellus, ac venenatis arcu wisi vel nisl. Vestibulum diam. Aliquam pellentesque, augue quis sagittis posuere, turpis lacus congue quam, in hendrerit risus eros eget felis. Maecenas eget erat in sapien mattis porttitor. Vestibulum porttitor. Nulla facilisi. Sed a turpis eu lacus commodo facilisis. Morbi fringilla, wisi in dignissim interdum, justo lectus sagittis dui, et vehicula libero dui cursus dui. Mauris tempor ligula sed lacus. Duis cursus enim ut augue. Cras ac magna. Cras nulla. Nulla egestas. Curabitur a leo. Quisque egestas wisi eget nunc. Nam feugiat lacus vel est. Curabitur consectetuer.

2. Monte Carlo methods

2.1. Monte Carlo integration

The canonical example of Monte Carlo sampling methods is the evaluation of multidimensional integrals of the form

$$\int f(\mathbf{R})p(\mathbf{R})d\mathbf{R} \tag{1}$$

Where $p(\mathbf{R})$ is a normalized probability distribution satisfying $\int p(\mathbf{R})d\mathbf{R} = 1$ and $p(\mathbf{R}) \geq 0$. We see that, at points where $p(\mathbf{R})$ is large, the value of $f(\mathbf{R})$ contributes more to the integral; as a result $p(\mathbf{R})$ is often referred to as an "importance function". In principle integrals of

the form (1) can be evaluated by carrying out an infinite sum:

$$\int f(\mathbf{R})p(\mathbf{R})d\mathbf{R} = \lim_{M\to\infty} \frac{1}{M} \sum_{\mathbf{R}\in\{\mathbf{R}\}_p} f(\mathbf{R}) \tag{2}$$

Where $\{\mathbf{R}\}_p$ is a set of M samples drawn from the distribution $p(\mathbf{R})$. In order to carry out these integrals in finite time we make the approximation that, for large M,

$$\int f(\mathbf{R})p(\mathbf{R})d\mathbf{R} \approx \frac{1}{M} \sum_{\mathbf{R}\in\{\mathbf{R}\}_p} f(\mathbf{R}) \tag{3}$$

We can then carry out the finite sum in (3) to obtain a numerical approximation to the integral in (1).

2.2. The metropolis algorithm

In Monte Carlo methods it is often necessary to draw samples from a distribution which is quite complicated (for example to generate $\{\mathbf{R}\}_p$ from $p(\mathbf{R})$ in equation 3). In order to do this we employ the *Metropolis algorithm*. This algorithm constructs a sequence of samples $\{\mathbf{R}_1, \mathbf{R}_2, ..., \mathbf{R}_N\}_p$ drawn from the distribution $p(\mathbf{R})$ by following a random walk:

1. Start the walker at a random position $\mathbf{R}$.
2. Generate a new position $\mathbf{R}_T$ from some transition probability density function $T(\mathbf{R} \to \mathbf{R}_T)$.
3. Accept the trail move (set $\mathbf{R} = \mathbf{R}_T$) with ("acceptance") probability

$$A(\mathbf{R} \to \mathbf{R}_T) = min\left(1, \frac{T(\mathbf{R}_T \to \mathbf{R})p(\mathbf{R}_T)}{T(\mathbf{R} \to \mathbf{R}_T)p(\mathbf{R})}\right) \tag{4}$$

4. Add $\mathbf{R}$ to our sample set.
5. loop steps $2 \to 4$ until N samples are generated.

In order to sample as efficiently as possible, the trial move transition probability $T(\mathbf{R} \to \mathbf{R}_T)$ should be chosen to maximize the proportion of trial moves which are accepted (the "acceptance"). We see that the best choice would be $T(\mathbf{R} \to \mathbf{R}_T) = p(\mathbf{R}_T)$, leading to $A(\mathbf{R} \to \mathbf{R}_T) = 1$ and 100% acceptance, but this would involve sampling trial moves directly from $p(\mathbf{R})$, the very problem we are trying to solve! In practice $T(\mathbf{R} \to \mathbf{R}_T)$ is chosen from a subset of transition probabilities which are easily sampled.

As can be readily seen from equation (4), the Metropolis algorithm is insensitive to the normalization of our distribution $p(\mathbf{R})$ (any normalization factor would simply cancel out in the division $p(\mathbf{R}_T)/p(\mathbf{R})$). This is an important advantage of the Metropolis algorithm as we may not know, or may not wish to calculate, the normalization of the distribution we are attempting to sample. This is often the case for complicated distributions in high-dimensional spaces (e.g many-body quantum-mechanical wavefunctions).

A demonstration that the choice of acceptance probability in (4) produces samples distributed according to $p(\mathbf{R})$ is given in [1] and reproduced here: Consider a large number of walkers all evolving according to the above rules. We assume that, after some equilibration period, the walkers settle down to a unique steady state distribution $n(\mathbf{R})$ so that the average number of walkers in the volume element $d\mathbf{R}$ is $n(\mathbf{R})d\mathbf{R}$. The average number of walkers moving from volume element $d\mathbf{R}$ to $d\mathbf{R}'$ in a single move will be:

$$A(\mathbf{R} \to \mathbf{R}')T(\mathbf{R} \to \mathbf{R}')n(\mathbf{R})d\mathbf{R}d\mathbf{R}' \tag{5}$$

In equilibrium this must be balanced by the number moving from $d\mathbf{R}'$ to $d\mathbf{R}$ $\implies$

$$A(\mathbf{R} \to \mathbf{R}')T(\mathbf{R} \to \mathbf{R}')n(\mathbf{R})d\mathbf{R}d\mathbf{R}' = A(\mathbf{R}' \to \mathbf{R})T(\mathbf{R}' \to \mathbf{R})n(\mathbf{R}')d\mathbf{R}'d\mathbf{R} \tag{6}$$

Hence

$$\frac{n(\mathbf{R})}{n(\mathbf{R}')} = \frac{A(\mathbf{R}' \to \mathbf{R})T(\mathbf{R}' \to \mathbf{R})}{A(\mathbf{R} \to \mathbf{R}')T(\mathbf{R} \to \mathbf{R}')} \tag{7}$$

By the choice of acceptance probability in (4) we have

$$\frac{A(\mathbf{R}' \to \mathbf{R})}{A(\mathbf{R} \to \mathbf{R}')} = \frac{T(\mathbf{R} \to \mathbf{R}')p(\mathbf{R})}{T(\mathbf{R}' \to \mathbf{R})p(\mathbf{R}')} \tag{8}$$

So that our equilibrium distribution satisfies

$$\frac{n(\mathbf{R})}{n(\mathbf{R}')} = \frac{p(\mathbf{R})}{p(\mathbf{R}')} \tag{9}$$

The equilibrium distribution $n(\mathbf{R})$ is therefore proportional to $p(\mathbf{R})$, and probability of finding any given walker in $d\mathbf{R}$ is then $p(\mathbf{R})d\mathbf{R}$ as required.

3. Variational quantum Monte Carlo

3.1. Introduction

Variational quantum Monte Carlo (VQMC) is the simplest quantum Monte Carlo method. It involves calculation of the variational energy:

$$E_V = \frac{\langle\psi_T|\hat{H}|\psi_T\rangle}{\langle\psi_T|\psi_T\rangle} = \frac{\int \psi_T^*(\mathbf{R})\hat{H}\psi_T(\mathbf{R})d\mathbf{R}}{\int|\psi(\mathbf{R})|^2 d\mathbf{R}} \tag{10}$$

Where $|\psi_T\rangle$ is a trial many-electron wave function and $\mathbf{R} = (\mathbf{r}_1, ..., \mathbf{r}_N)$ is an electronic configuration. In

VQMC the integrals in (10) are evaluated directly using the Monte Carlo integration techniques described in section 2. In order to do this we rewrite (10) as

$$E_V = \frac{\int |\psi(\mathbf{R})|^2 \psi_T(\mathbf{R})^{-1} \hat{H} \psi_T(\mathbf{R}) d\mathbf{R}}{\int |\psi(\mathbf{R})|^2 d\mathbf{R}} = \int p(\mathbf{R}) E_L(\mathbf{R}) d\mathbf{R} \quad (11)$$

Where we have defined an "importance function",

$$p(\mathbf{R}) = \frac{|\psi(\mathbf{R})|^2}{\int |\psi(\mathbf{R})|^2 d\mathbf{R}} \quad (12)$$

And a "local energy",

$$E_L(\mathbf{R}) = \psi_T^{-1}(\mathbf{R}) \hat{H} \psi_T(\mathbf{R}) \quad (13)$$

Employing (3) we may then approximate E_V as

$$E_V \approx \frac{1}{M} \sum_{\mathbf{R} \in \{\mathbf{R}\}_p} E_L(\mathbf{R}) \quad (14)$$

Where $\{\mathbf{R}\}_p$ is a set of M samples drawn from the distribution $p(\mathbf{R})$. These samples are obtained using the Metropolis algorithm (see section 2.2).

3.1.1. The variational principle

The variational energy E_V is bounded from below by the ground state energy of our system E_0. This is known as the *variational principle*. This can be readily seen by expanding $|\psi_T\rangle$ as $|\psi_T\rangle = \sum_n \alpha_n |n\rangle$ where $\{|n\rangle\}$ are the (orthonormal) eigenstates of $\hat{H}$ such that $\hat{H}|n\rangle = E_n |n\rangle$ and $\{\alpha_n\}$ are expansion coefficients. Then

$$E_V = \frac{\langle \psi_T | \hat{H} | \psi_T \rangle}{\langle \psi_T | \psi_T \rangle} = \frac{\sum_{n,m} \alpha_n \alpha_m^* \langle m | \hat{H} | n \rangle}{\sum_{n,m} \alpha_n \alpha_m^* \langle m | n \rangle} \quad (15)$$

$$= \frac{\sum_n |\alpha_n|^2 E_n}{\sum_n |\alpha_n|^2} \geq E_0 \ \forall \ \{\alpha_n\} \quad (16)$$

Where we have used

$$\langle m | n \rangle = \delta_{m,n} \quad (17)$$

$$\langle m | \hat{H} | n \rangle = \delta_{m,n} E_n \quad (18)$$

$$E_n \geq E_0 \ \forall \ n \quad (19)$$

This means that if we parameterize our trial wavefunction as $|\psi_T\rangle = |\psi_T(\mathbf{c})\rangle$, where $\mathbf{c}$ is some parameter set, then the best approximation to our ground state is when E_V is minimized. This constitutes a method of estimating the ground state and ground state energy for arbitrary systems given some model parameterization $|\psi_T(\mathbf{c})\rangle$.

3.1.2. Energy variance

Another interesting quantity which we may wish to calculate is the variance in the set of local energies evalueated at our configuration samples. This variance not only provides the standard error in our variational energy, but also provides additional information about our trial wavefunction; If the trial wavefunction is an exact eigenstate of the Hamiltonian, i.e a solution to the Schrödinger equation:

$$\hat{H} |\psi_T\rangle = E |\psi_T\rangle \quad (20)$$

Then both the variational and the local energy become trivial:

$$E_L(\mathbf{R}) = \psi(\mathbf{R})^{-1} \hat{H} \psi(\mathbf{R}) = \psi(\mathbf{R})^{-1} E \psi(\mathbf{R}) = E \quad (21)$$

$$E_V = \frac{\langle \psi_T | \hat{H} | \psi_T \rangle}{\langle \psi_T | \psi_T \rangle} = \frac{\langle \psi_T | E | \psi_T \rangle}{\langle \psi_T | \psi_T \rangle} = E \quad (22)$$

Hence there is no variance in the local energies. As a result, minimisation of the variance will take our trial wavefunction towards eigenstates of the Hamiltonian. However, we must be careful when evaluating the variance of our local energies. Due to the sequential nature of the metropolis algorithm our sampled configurations are serially correlated; each sampled point depends on the previous one ($T(\mathbf{R} \to \mathbf{R}')$ depends on $\mathbf{R}$). As a result successive local energies will be more similar on average than if the configurations were uncorrelated, artificially reducing the variance of our local energies. The *reblocking method* can be used to correct for this correlation and give an unbiased estimate of the variance, it is described in section 3.1.3.

3.1.3. The reblocking method

Our sequence of configurations will have some correlation length over which knowledge of previous configurations is lost (measured in Monte Carlo steps). As a result our local energies will also be correlated, leading to an artificial reduction in the local energy variance. The *reblocking method* corrects for this by gathering successive local energies into blocks and averages over each block (this is known as a *blocking transformation*). If the block length, L_B, is greater than the correlation length, the block averages will then be uncorrelated and can be used to construct the unbiased "reblocked" variance:

$$\sigma_B^2 = \frac{1}{1 - N_B} \sum_b (E_b - E_V)^2 \quad (23)$$

Where $N_B = M/L_B$ is the number of blocks (not necessarily an integer as M might not be a multiple of $L_B \Leftrightarrow$

the last block might be incomplete) and E_b is the averaged energy of the b^{th} block, B_b, which contains N_b samples:

$$E_b = \frac{1}{N_b} \sum_{\mathbf{R} \in B_b} E_L(\mathbf{R}) \tag{24}$$

3.2. Implementation

The following VQMC calculations are carried out using a FORTRAN code which takes as input a set of nucleii, a set of (suitably chosen) single-electron basis functions $\{\phi_n(\mathbf{r})\}$ and the number of spin-up and spin-down electrons (N_u and N_d respectively). The program is also provided with $N = N_u + N_d$ sets of basis coefficients, or *characters*, c_{in} that describe N single particle states $\psi_i(\mathbf{r})$ as an expansion in our basis:

$$\psi_i(\mathbf{r}) = \sum_n c_{in} \phi_n(\mathbf{r}) \tag{25}$$

In a more complete treatment, the Hartree-Fock problem would be solved in the basis $\{\phi_n(\mathbf{r})\}$ and $\{\psi_i(\mathbf{r})\}$ would be the resulting Hartree-Fock orbitals. However, this is not necassary to investigate the important aspects of VQMC, and in our calculations we simply provide reasonable physically motivated characters c_{in}, we will see that this still gives very sensible results. The single particle states $\{\psi_i(\mathbf{r})\}$ are then used to construct the trial many-body wavefucntion $\psi_T(\mathbf{R})$ from which the variational energy E_V is calculated. We explain this construction in section 3.2.2.

3.2.1. Basis sets

The VQMC calculations are carried out using an atomic basis set of hydrogen-like orbitals:

$$\phi_{nlmz}(\mathbf{r}) = \mathcal{N} e^{-Zr/na_0} \left(\frac{2Zr}{na_0}\right)^l L^{2l+1}_{n-l-1}\left(\frac{2Zr}{na_0}\right) Y_{lm}(\theta, \phi) \tag{26}$$

Where

$$\mathcal{N} = \sqrt{\left(\frac{2Z}{na_0}\right)^3 \frac{(n-l-1)!}{2n[(n+l)!\,]}} \tag{27}$$

is a normalization constant, $L^\alpha_n(x)$ is a generalized Laguerre polynomial, $Y_{lm}(\theta, \phi)$ is a spherical harmonic, Z is the nuclear charge and a_0 is the bohr radius (≈ 0.529Å). The particular values of n, l, m, z included in our basis are chosen to best describe the system in question.

3.2.2. Trial wavefunction construction

Our VQMC code constructs a trial many-body wavefunction $\psi_T(\mathbf{R})$ from our single-electron states $\{\psi_i(\mathbf{r})\}$. The wavefunction is of the Slater-Jastrow form:

$$\psi_T(\mathbf{R}, \mathbf{b}) = J(\{r_{ij}\}, \mathbf{b}) \begin{vmatrix} \psi_1(\mathbf{r}_1) & \dots & \psi_1(\mathbf{r}_N) \\ \vdots & & \vdots \\ \psi_N(\mathbf{r}_1) & \dots & \psi_N(\mathbf{r}_N) \end{vmatrix} \tag{28}$$

$$= J(\{r_{ij}\}, \mathbf{b})\, S(\{\mathbf{r}_i\}) \tag{29}$$

Where $\{r_{ij}\}$ is the set of electron-electron and electron-nuclear separations, $J(\{r_{ij}\}, \mathbf{b})$ is a Jastrow factor with variational parameters $\mathbf{b}$ and $S(\{\mathbf{r}_i\})$ is the Slater determinant constructed from our single particle states $\{\psi_i(\mathbf{r})\}$. The Slater determinant ensures the correct exchange antisymmetry and the Jastrow factor approximates electron-electron correlation effects.

3.2.3. The Jastrow factor

Our trial wavefunction (equation 28) includes a Jastrow factor to model the effects of electron correlation. The functional form of the Jastrow factor is heuristically motivated to recover as much of the correlation energy as possible. One way to achive this is to engineer the Jastrow factor so that the wavefunction obeys the *electron cusp conditions* (see appendix A). These are a set of conditions on the derivatives of the wavefunction near charge centres that are a direct result of the Schrödinger equation. These include the nuclear-electron cusp and the like and unlike spin electron-electron cusps. We use a Jastrow factor that explicitly satisfies the cusp conditions:

$$J(\{r_{ij}\}) = exp\left(\sum_{i<j} U_{ij}\right) \tag{30}$$

Where the Jastrow correlations factors U_{ij} are defined as

$$U_{ij} = \frac{a_{ij} r_{ij}}{1 + b_{ij} r_{ij}} \tag{31}$$

where $r_{ij} = |\mathbf{r}_i - \mathbf{r}_j|$,

$$a_{ij} = \begin{cases} 1 & \text{if i, j are like spin electrons} \\ 2 & \text{if i, j are unlike spin electrons} \\ 4 & \text{if i, j is an electron nuclear pair} \end{cases} \tag{32}$$

and b_{ij} are variational parameters. The form of a_{ij} is due to the different forms of the electron cusp conditions when different species are involved (see appendix A).

3.2.4. Wavefunction sampling

The wavefunction in equation 28 is sampled using the metropolis algorithm (see section 2.2) with the trial moves in configuration space consisting of moving a randomly chosen electron by some random displacement between 0 and 4Å in a random direction. Figure 1 demonstrates the results of this sampling for single electrons in atomic 2p and 5d states.

We see that, as expected, the quality of the reproduction of the electron density increases with the number of Metropolis samples. It can also be seen that the 5d state requires more samples to be reasonably well described, illustrating the general point that more samples are required as the complexity of the wavefunction increases. This effect is compounded as the dimensionality of the wavefunction increases with increasing numbers of electrons.

One important factor in achieving good sampling is achieving ergodicity, ensuring that all important regions of configuration space can, and will, be visited by the algorithm. Figure 1 illustrates some of the negative effects of poor ergodicity. For the 5d orbital, when only 10^4 samples are generated (bottom row, 2^{nd} from the left), the algorithm spends a disproportionate amount of time in the upper half of the plane, causing a fictitious electron polarization. This is because it is having a hard time penetrating the horizontal barrier of low electron density at $z = 0$, resulting in an average time to make the jump through $z = 0$ that is comparable to the simulation time. As a result it is more likely that there will be a difference between the number of steps spent above the barrier and the number spent below, leading to biased sampling. Situations like this are why a reasonably large maximum electron jump distance of 4Å was chosen; it is important that the electrons penetrate such barriers often during the sampling in order to ensure spatially disconnected regions of electron density are sampled proportionally. In order to achive this, they must be allowed to jump directly between these 'islands' of high electron density, as small steps from one island towards another will end up in the intermediate regions of low electron density and likely be rejected, leading to the algorithm becoming stranded on one island.

4. Results

4.1. Hydrogen

4.1.1. Ground state calculations

The simplest system to model is the Hydrogen atom as it has only one electron in a simple one-proton potential. This system has an analytic solution with energy levels $E_n = -\mathcal{R}/n^2$ where $\mathcal{R}$, the Rydberg constant, is one of the most accurately measured physical constants, with a defined value of 0.5 Hartree (≈13.605693009 eV). The ground state energy of the Hydrogen atom is therefore $E_1 = -\mathcal{R}$. The ground state wavefunction is the atomic 1s state for a charge 1 nucleus, $\psi_{1s,z=1}(\mathbf{r}) \propto exp(-r/a_0)$, where a_0 is the Bohr radius and takes the value $a_0 = 0.529177$ Å.

Because hydrogen has this analytic solution, it serves as a good test for our VQMC code as we can use just the 1s state as our only single particle state. As a result our Jastrow factor is 1 and our Slater determinant becomes the trivial 1×1 case. The resulting trial wavefunction is then $\psi_T(\mathbf{r}) = \psi_{1s,z=1}(\mathbf{r})$, the exact ground state. Both the variational energy and the local energy (evaluated anywhere) should then be $-\mathcal{R}$ (see section 3.1.2).

With this in mind we carry out a VQMC simulation of the hydrogen atom with $\psi_T(\mathbf{r}) = \psi_{1s,z=1}(\mathbf{r})$, and 10^7 sample electron locations. Figure 2 shows the error in local energy (i.e $E_L + \mathcal{R}$) for these sampled electron positions.

We see that the vast majority of local energies lie within approximately $1.8{\times}10^{-7}$ Hartree (∼ 5 μeV) of the correct value of $-\mathcal{R}$. The resulting variational energy (⇔ average local energy) is E_V = -0.49999997027 Hartree (-13.6056922 eV), $2.973{\times}10^{-8}$ Hartree (∼ 0.75 μeV) above the theoretical value.

4.1.2. Exited state mixing

Our single particle states $\{\psi_i(\mathbf{r})\}$ in section 4.1.1 consisted of only the exact ground state. However, it is interesting to look at the results of calculations with states which are not the exact ground state. To this end we perform a series of VQMC simulations with the trial wavefunction set to an interpolation between the n^{th} and $n + 1^{th}$ S state of hydrogen:

$$\psi_T(\mathbf{r}) = c_1\,\psi_{ns,z=1}(\mathbf{r}) + c_2\,\psi_{(n+1)s,z=1}(\mathbf{r}) \tag{33}$$

Once again, since we are only dealing with one electron the slater determinant becomes trivial and the Jastrow factor is 1. For each n we run a VQMC simulation for a series of real valued coefficients such that

$$c_1 \in [0, 1] \tag{34}$$

$$c_2 = 1 - c_1 \tag{35}$$

And define an effective (continuous) quantum number $n_{eff} = n + c2$, which measures our progress up the series of hydrogen S states $\{1s, 2s, 3s, 4s...\}$. For example an equal mixing of 3s and 4s states would correspond to $n_{eff} = 3.5$. At integer values of n_{eff} we recover exact eigenstates and so expect the energy to evaluate to

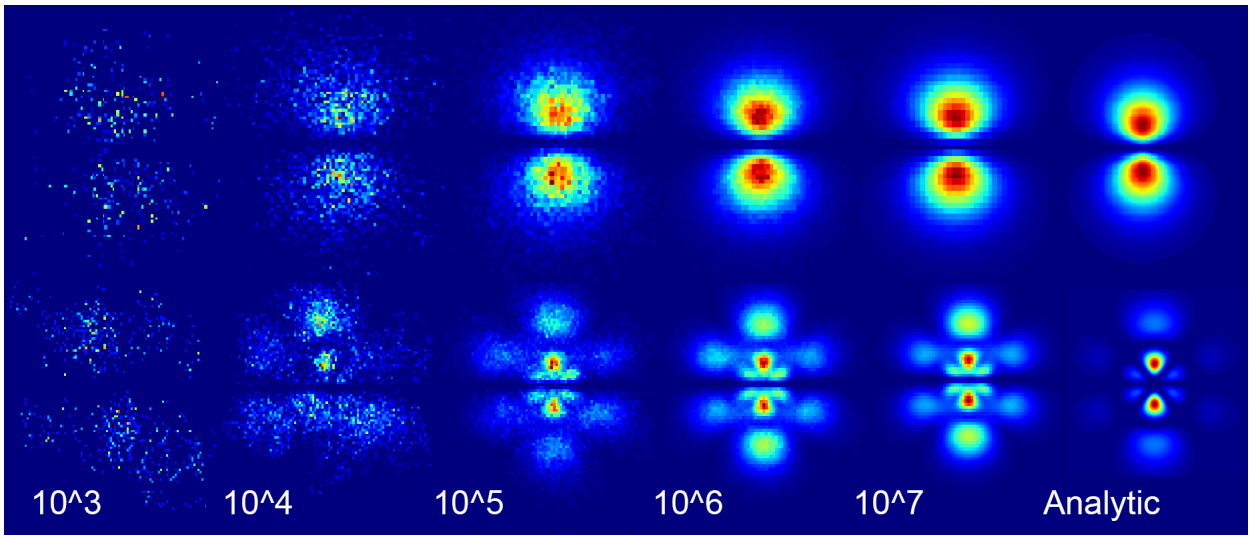

Figure 1: x-z plane of the Metropolis sampling of atomic 2p (upper) and 5d (lower) states. The 2p state was sampled with the quantum numbers $n = 2$, $l = 1$ and $m = 1$ and the 5d with $n = 5$, $l = 2$ and $m = 1$. The nuclear charge was $z = 1$ in both cases. The states are labelled with the number of samples generated and the analytic electron density is included (far right) for comparison.

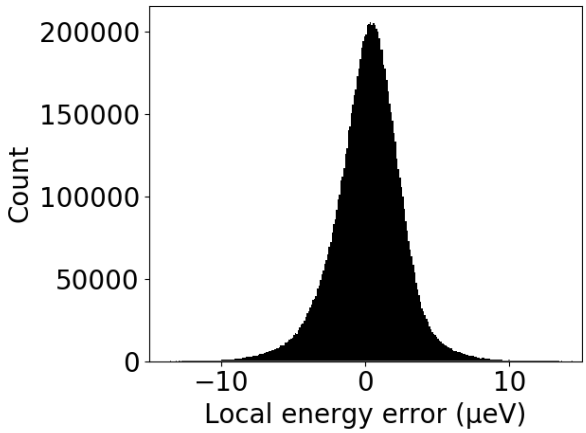

Figure 2: Error in local energies for the exact hydrogen ground state (10^7 samples total). Average local energy = E_V = -0.49999997027 Hartree (-13.6056922 eV).

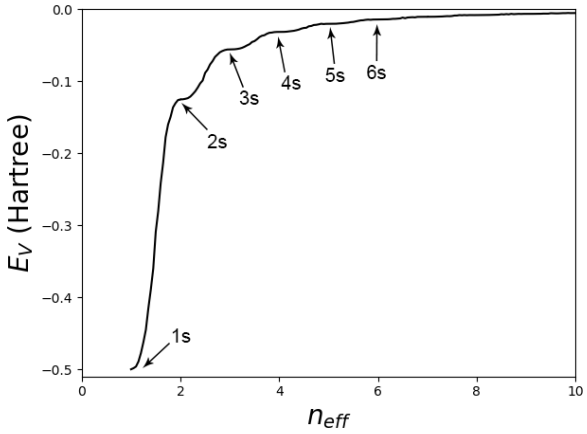

Figure 3: The variational energy of hydrogen for mixed S states. n_{eff} corresponds to the interpolation between neighbouring S states (i.e $n_{eff} = 3.5$ corresponds to a linear combination of 3s and 4s states with equal weights). Each data point was calculated using 10^5 sampled electron configurations ($\Leftrightarrow$ metropolis Monte Carlo iterations).

$-\mathcal{R}/n_{eff}^2$ and the variance to go to 0. The energy and reblocked variance (see section 3.1.3) are plotted against $n_eff \in [1, 10]$ in figures 3 and 4 respectively.

We see that the behaviour is as expected. The variational energy (figure 3) plateaus near integer values of n_{eff} to the corresponding hydrogenic energy level $-\mathcal{R}/n_{eff}^2$. The n_{eff}^{-2} energy scaling is clear to see, as well as the asymptotic approach to the continuum states as $n_{eff} \to \infty$. The reblocked variance (figure 4) sharply decreases near integer values of n_{eff} as expected from section 3.1.2.

4.1.3. The H_2^+ ion

The next most complicated system that we can study using our VQMC code is the H_2^+ ion consisting of two protons and one electron. In order for this system to be stable and to not simply dissociate into a free proton and a Hydrogen atom there must exist an energy minima, E_{min}, at some finite value of the proton-proton separation, R, the H_2^+ bond length. The dissociated energy is simply the energy of the free Hydrogen atom, $-\mathcal{R}$, and

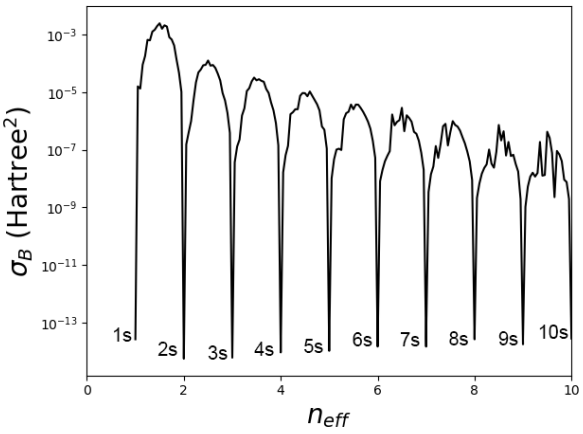

Figure 4: The reblocked local energy variance of hydrogen for mixed S states. n_{eff} is defined as in figure 3. Each data point was calculated using 10^5 sampled electron configurations ($\Leftrightarrow$ metropolis Monte Carlo iterations) and a reblocking length is $L_B = 1000$. Note the log scale on the y axis.

so the E_{min} should be given by $E_{min} = -\mathcal{R} - E_{bind}$, where E_{bind} is the H_2^+ binding energy. An analytic solution for this system exists [2] and gives $E_{bind} = 0.1026346191$ Hartree (2.79283 eV) and R = 1.056869267 Å.

We employ a simple model of the H_2^+ ion, placing the first proton at the origin and the second at some displacement, δ, along the z axis. Our electronic model consists of a a linear combination of hydrogenic 1s orbitals localized at each proton:

$$\psi_T(\mathbf{r}) = a\,\psi_{1s,z=1}(\mathbf{r}) + b\,\psi_{1s,z=1}(\mathbf{r} - \delta\hat{\mathbf{z}}) \qquad (36)$$

A simple quantum-mechanical treatment (see appendix B) shows that the 1s orbitals hybridize under the action of the Hamiltonian to form two molecular orbitals, the bonding ($a = b$) and anti-bonding ($a = -b$) orbitals. The bonding orbital has a higher electron density between the protons (the 1s orbitals sum constructively, rather than destructively), screening the protons from one another, and forming a covalent bond; this can be seen in an example metropolis sampling of the bonding and antibonding orbitals in figure 5. As a result, the bonding orbital is the lower energy state and exhibits the energy minima required for stability of the H_2^+ ion. Once again because this is a single-electron system our slater determinant is trivial and our Jastrow factor is 1.

We run a series of VQMC simulations for a range of bond lengths $\delta \in [0,10]$Å, using 10^5 Metropolis Monte Carlo iterations at each. The resulting energy landscape is shown in figure 6. The bonding orbital exhibits the energy minima required for stability of the H_2^+ ion, and both orbitals show the correct asymptotic behavior of

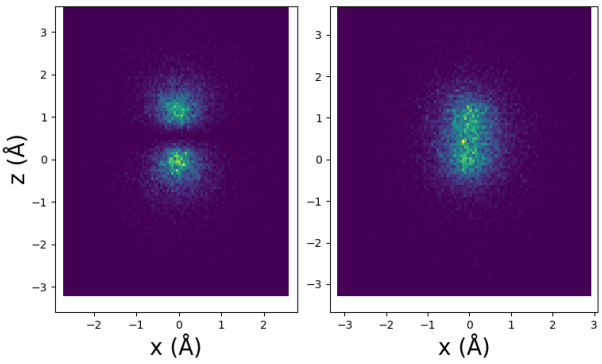

Figure 5: The Metropolis sampled electron positions (in the x-z plane) for the bonding (right) and anti-bonding (left) orbitals of a H_2^+ ion, constructed from hydrogenic 1s states. 10^5 Metropolis samples were generated.

$E_V \to -\mathcal{R}$ as $\delta \to \infty$. This model gives predicted values $R = 1.240$Å and $E_{bind} = 0.068$ Hartree (1.8523 eV). These values are sensible, but reasonably removed from the analytic solution. This is due to the fact that our electronic basis provides an incomplete description of the electronic state. This is more prominent in molecular systems as we are using the basis of atomic orbitals, with no modifications to allow for delocalization or polarization of the electron density.

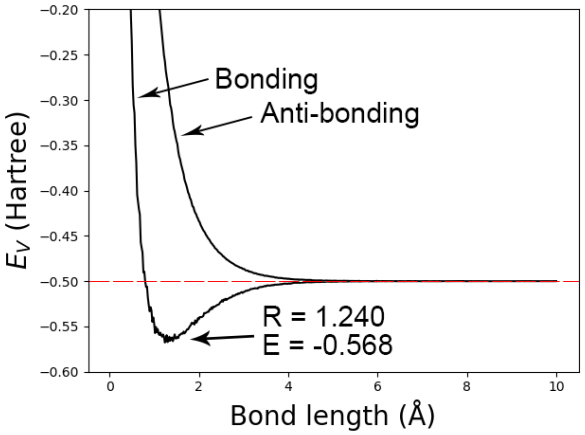

Figure 6: The variational energy vs bond length of a H_2^+ ion in the hybridized 1s bonding and anti-bonding orbitals. The energy minima of the bonding orbital can clearly be seen, accounting for the stability of the H_2^+ ion. As $R \to \infty$, $E_v \to -\mathcal{R}$ for both orbitals, which corresponds to the dissociation of the H_2^+ ion into a Hydrogen atom and free proton. 10^5 Metropolis Monte Carlo iterations were used for each data point, the same as was used to produce figure 5.

4.1.4. The H_2 molecule

So far all of the systems investigated contained only one electron. As a result our Slater-Jastrow wavefunction simply became a simple single-electron wavefunction. We now move on to multi-electron systems, the first of which is the H_2 molecule. A crude model of the H_2 molecule consists of simply adding another electron (of opposing spin) into the bonding orbital of the H_2^+ ion. Because different spin electrons are distinguishable, the spatial part of the Slater Determinant factorizes into a part associated with up electrons and a part associated to down electrons (our code does this implicitly). For example, if we denote the bonding orbital as $\beta(\mathbf{r})$, in our crude H_2 model the spatial part of the Slater determinant becomes the simple product state $\beta(\mathbf{r}_1)\beta(\mathbf{r}_2)$:

$$\psi_T(\mathbf{r}_1, \mathbf{r}_2) = J(\{r_{ij}\}) \begin{vmatrix} \beta(\mathbf{r}_1)|\uparrow_1\rangle & \beta(\mathbf{r}_2)|\uparrow_2\rangle \\ \beta(\mathbf{r}_1)|\downarrow_1\rangle & \beta(\mathbf{r}_2)|\downarrow_2\rangle \end{vmatrix} \tag{37}$$

$$= J(\{r_{ij}\})\beta(\mathbf{r}_1)\beta(\mathbf{r}_2)(|\uparrow_1\downarrow_2\rangle - |\uparrow_2\downarrow_1\rangle) \tag{38}$$

Since our Hamiltonian has no spin dependence, the calculation is the same as one performed with the effective trial wavefunction:

$$\psi_T(\mathbf{r}_1, \mathbf{r}_2) = J(\{r_{ij}\})\beta(\mathbf{r}_1)\beta(\mathbf{r}_2) \tag{39}$$

So, for this model of H_2, we are dealing with a simple product state with a multiplicative Jastrow factor. As a result, this system provides a good test bench for the effectiveness of our Jastrow factor. We carry out a similar calculation as we did with the H_2^+ ion; running a series of VQMC calculations at a range of H-H bond lengths. We use both a parameterless Jastrow factor ($b_{ij} = 1 \; \forall \; i, j$) and a simple Slater determinant (i.e with the Jastrow factor set to 1). The resulting variational energy landscape is plotted in figure 7.

We see that the Slater-Jastrow wavefunction typically results in lower energies, even without parameter tuning. This is to be expected because he electron cusp conditions are now enforced and the resulting wavefunction behaves more correctly where charges come together (i.e both when the electrons are near the nucleii and when they are near each other). Unfortunately the only place where the parameterless Jastrow factor behaves poorly is near the crucial energy minima, resulting in a worse estimate for the ground state energy and bond length. It is not particularly surprising that a parameterless Jastrow factor will not work over the whole range of bond lengths, but it is unfortunate that it performs worse in this key region. It is also interesting to note the erratic behaviour of the variational energy at large bond lengths. This is actually expected behaviour and is the result of the breakdown of our Metropolis sampling as the two regions of electron density (around the two nucleii) become isolated from one another. This will result in each electron becoming biased towards (or even trapped on) a particular nucleus, despite the fact that it's wavefunction, $\beta(\mathbf{r})$, is unbiased to either (see the discussion in section 3.2.4). As a result, when both electrons are bias towards a particular nucleus, the energy spikes due to additional electron-electron repulsion. This also explains why the onset of this effect occurs above 4Å, as this is the maximum electon jump distance used in our Metropolis algorithm.

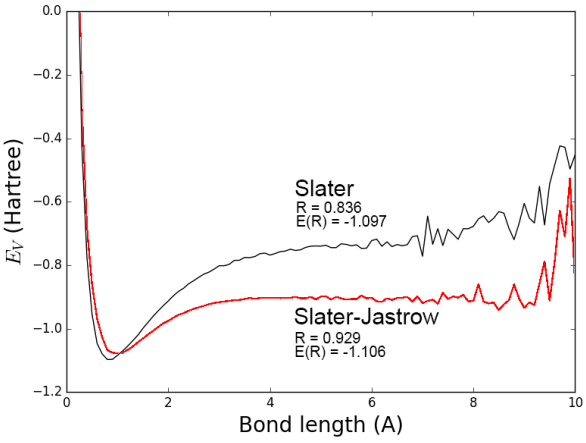

Figure 7: The variational energy vs bond length for a H_2 molecule with two electrons in the bonding orbital. Each point was calculated using 10^5 Metropolis Monte Carlo iterations. The results for both a Slater and a parameterless Slater-Jastrow wavefunction are shown, along with the predicted minimum energy and corresponding bond length.

4.2. Helium

The next multi-electron system that we investigate is the Helium atom. Helium consists of a charge-2 nucleus and two electrons, with an experimentally determined ground state energy of -2.903386 Hartree (-79.00515 eV) [3]. In order to model Helium We provide our VQMC code with two 1s orbitals, one spin up and one spin down. As explained in section 4.1.4, this means that our Slater determinant becomes spatially trivial:

$$\psi_T(\mathbf{r}_1, \mathbf{r}_2) = J(\{r_{ij}\}) \begin{vmatrix} \psi_{1s,z=2}(\mathbf{r}_1)|\uparrow_1\rangle & \psi_{1s,z=2}(\mathbf{r}_2)|\uparrow_2\rangle \\ \psi_{1s,z=2}(\mathbf{r}_1)|\downarrow_1\rangle & \psi_{1s,z=2}(\mathbf{r}_2)|\downarrow_2\rangle \end{vmatrix} \tag{40}$$

$$= J(\{r_{ij}\})\psi_{1s,z=2}(\mathbf{r}_1)\psi_{1s,z=2}(\mathbf{r}_2)(|\uparrow_1\downarrow_2\rangle - |\uparrow_2\downarrow_1\rangle) \tag{41}$$

And similarly to section 4.1.4, since our Hamiltonian has no spin dependence, the calculation is the same as

one performed with the effective trial wavefunction:

$$\psi_T(\mathbf{r}_1, \mathbf{r}_2) = J(\{r_{ij}\})\psi_{1s,z=2}(\mathbf{r}_1)\psi_{1s,z=2}(\mathbf{r}_2) \qquad (42)$$

Helium therefore serves as another good test of our Jastrow factor. We carry out a VQMC simulation of Helium, using the wavefunction given in equation 40, with 10^7 Metropolis Monte Carlo iterations. We use the same parameterless Jastrow factor as in section 4.1.4 and once again compare with the bare Slater determinant case. The results are show in table 1.

Table 1: Helium energies

Method	Variational energy (Hartree)
Slater	-2.745244
Slater-Jastrow	-2.862630

We see that even without parameter tuning, our Slater-Jastrow wavefunction has recovered much of the correlation energy of our system (even with a minimal basis). As in section 4.1.4, this is due to the fact that the electron cusp conditions are now enforced and the resulting wavefunction behaves more correctly where charges come together.

4.3. Lithium to Boron

So far none of the systems that we have investigated have a non-trivial Slater determinant, simply because we have been dealing with ≤ 2 electrons, where the electrons will naturally assume opposite spins in order to occupy lower energy single-particle states. In this section we investigate a series of systems that use all of the factors in our trial wavefunction (equation 28) in a non-trivial way, providing a rigorous test of all of the elements involved. This also allows us to investigate the scaling properties of our code. The simplest choice of test cases is atomic systems with $Z \geq 3$. We model these systems by using as our single particle states the relevant uncorrelated ground state configuration ($1s^2 2s^2 2p^6 ...$), populated according to Hund's rules. According to equation 28, this is then antisymmetrised using a Slater determinant and a parameterless Jastrow factor ($b_{ij} = 1 \; \forall \; i, j$) is applied. The results are summarized in table 2. The previous results for Hydrogen and Helium are also included for completeness. Table 3 gives performance information for these systems on a 4 core 2.8GHz laptop (the same one used to run all of the simulations for this report).

We see that very reasonable energies are calculated, despite using the simple uncorrelated electronic states as our starting point. It is also interesting to note that a value of -24.546707 Hartree for the variational energy of Boron is reported in [7] using VQMC with an optimized five-parameter trial wave function. The fact that our answer isn't hugely removed from this suggests that using the uncorrelated states as a starting point was not complete garbage.

Table 2: Atomic system energies

System	Z	E_V (Hartree)	E (Hartree)
Hydrogen	1	-0.500000	-0.500000
Helium	2	-2.862630	-2.903386 [3]
Lithium	3	-7.300370	-7.477943 [4]
Beryllium	4	-14.32830	-14.66735 [5]
Boron	5	-23.42837	-24.65393 [6]

The calculated variational energies (E_V) of a succession of atomic systems. Here E is the value given in the literature.

Table 3: Atomic system performance

System	Z	t_i (μs)	$10^7 t_i$
Hydrogen	1	3.672	37s
Helium	2	20.68	3m 27s
Lithium	3	75.51	12m 35s
Beryllium	4	161.4	26m 54s
Boron	5	735.3	2h 2m 33s

The time taken per Metropolis Monte Carlo iteration (t_i) for a series of atomic calculations on a 2.8GHz quad-core laptop. These were measured using 10^7 total iterations, for which the total time is also given.

On the other hand, the performance leaves much to be desired; taking a few hours to calculate the energies of reasonably small atomic systems. This is to be expected as very little time was spent optimizing the routines used, apart from the relatively trivial parallelisation (which is near perfect due to the nature of Monte-Carlo calculations). About half of the CPU time was spent simply evaluating the atomic orbitals, probably because their values were recalculated every time they were evaluated, rather than storing previous results.

5. Conclusions

Fusce mauris. Vestibulum luctus nibh at lectus. Sed bibendum, nulla a faucibus semper, leo velit ultricies tellus, ac venenatis arcu wisi vel nisl. Vestibulum diam. Aliquam pellentesque, augue quis sagittis posuere, turpis lacus congue quam, in hendrerit risus eros eget felis. Maecenas eget erat in sapien mattis porttitor. Vestibulum porttitor. Nulla facilisi. Sed a turpis eu lacus commodo facilisis. Morbi fringilla, wisi in dignissim

interdum, justo lectus sagittis dui, et vehicula libero dui cursus dui. Mauris tempor ligula sed lacus. Duis cursus enim ut augue. Cras ac magna. Cras nulla. Nulla egestas. Curabitur a leo. Quisque egestas wisi eget nunc. Nam feugiat lacus vel est. Curabitur consectetuer.

Acknowledgements

Fusce mauris. Vestibulum luctus nibh at lectus. Sed bibendum, nulla a faucibus semper, leo velit ultricies tellus, ac venenatis arcu wisi vel nisl. Vestibulum diam. Aliquam pellentesque, augue quis sagittis posuere, turpis lacus congue quam, in hendrerit risus eros eget felis. Maecenas eget erat in sapien mattis porttitor. Vestibulum porttitor. Nulla facilisi. Sed a turpis eu lacus commodo facilisis. Morbi fringilla, wisi in dignissim interdum, justo lectus sagittis dui, et vehicula libero dui cursus dui. Mauris tempor ligula sed lacus. Duis cursus enim ut augue. Cras ac magna. Cras nulla. Nulla egestas. Curabitur a leo. Quisque egestas wisi eget nunc. Nam feugiat lacus vel est. Curabitur consectetuer.

A. Electronic cusp conditions

We derive a condition on the form of an electronic wavefunction in the vicinity of a charge centre known as the *electronic cusp condition*. We begin by considering the form of the Schrödinger equation in the vicinity of a charge, Z, at the origin (in atomic units):

$$\left(-\frac{1}{2}\nabla^2 - \frac{Z}{r}\right)\psi(\mathbf{r}) = E\psi(\mathbf{r}) \tag{43}$$

We then split the laplacian into the radial part ∇_r^2 and the angular part $\nabla_{\theta,\phi}^2$:

$$\left(-\frac{1}{2}(\nabla_r^2 + \nabla_{\theta,\phi}^2) - \frac{Z}{r}\right)\psi(\mathbf{r}) = E\psi(\mathbf{r}) \tag{44}$$

Averaging this equation over the angular degrees of freedom we then have

$$\left(-\frac{1}{2}\nabla_r^2 - \frac{Z}{r}\right)\overline{\psi}(\mathbf{r}) = E\overline{\psi}(\mathbf{r}) \tag{45}$$

where $\overline{\psi}(\mathbf{r})$ denotes the angular average of $\psi(\mathbf{r})$. Writing the radial laplacian explicitly we then have:

$$\left(-\frac{1}{2}\frac{1}{r^2}\left(2r\frac{\partial}{\partial r} + r^2\frac{\partial^2}{\partial r^2}\right) - \frac{Z}{r}\right)\overline{\psi}(\mathbf{r}) = E\overline{\psi}(\mathbf{r}) \tag{46}$$

separating out the $\frac{1}{r}$ terms:

$$-\frac{1}{r}\left(\frac{\partial}{\partial r} + z\right)\overline{\psi}(\mathbf{r}) - \frac{1}{2}\frac{\partial^2}{\partial r^2}\overline{\psi}(\mathbf{r}) = E\overline{\psi}(\mathbf{r}) \tag{47}$$

In the limit $r \to 0$ the first term dominates and so must independently vanish $\implies$

$$\lim_{r\to 0}\left(\frac{\partial\overline{\psi}(\mathbf{r})}{\partial r} + z\overline{\psi}(\mathbf{r})\right) = 0 \tag{48}$$

This is the electronic cusp condition. When the charge centre is a nucleus the condition is exactly as above, however there also exists a cusp condition when the charge centre is another electron. For two (opposite spin) electrons there are two kinetic terms, leading to a factor of 2 in front of the derivative term and so the unlike spin electron electron cusp condition reads:

$$\lim_{r_{12}\to 0}\left(2\frac{\partial\overline{\psi}(\mathbf{r}_1,\mathbf{r}_2)}{\partial r_{12}} - \overline{\psi}(\mathbf{r}_1,\mathbf{r}_2)\right) = 0 \tag{49}$$

where r_{12} is the separation between electrons 1 and 2. For same spin electrons a further factor of 2 is introduced due to the echange antisymmetry of the wavefunction; however the antisymmetry requirement keeps the electrons away from one another anyway and imposing the like-spin cusp condition at $\mathbf{r}_1 = \mathbf{r}_2$ has little affect on the electronic energy/variance [8]. These arguments can be generalized to give the full many-electron cusp conditions:

$$\lim_{r_{ij}\to 0}\left(\frac{\partial\overline{\psi}(\mathbf{R})}{\partial r_{ij}} + z_j\overline{\psi}(\mathbf{R})\right) = 0 \text{ (electron i, nucleus j)} \tag{50}$$

$$\lim_{r_{ij}\to 0}\left(2\frac{\partial\overline{\psi}(\mathbf{R})}{\partial r_{ij}} - \overline{\psi}(\mathbf{R})\right) = 0 \text{ (unlike-spin electrons i, j)} \tag{51}$$

$$\lim_{r_{ij}\to 0}\left(4\frac{\partial\overline{\psi}(\mathbf{R})}{\partial r_{ij}} - \overline{\psi}(\mathbf{R})\right) = 0 \text{ (like-spin electrons i, j)} \tag{52}$$

B. Bonding and Anti-bonding in H_2^+

In section 4.1.3 we investigated the properties of the H_2^+ ion by considering an electronic state of the form

$$\psi_T(\mathbf{r}) = a\,\psi_{1s,z=1}(\mathbf{r}) + b\,\psi_{1s,z=1}(\mathbf{r} - \delta\hat{\mathbf{z}}) \tag{53}$$

Where $\delta\hat{\mathbf{z}}$ is the position of the second proton. We can re-write this in bra-ket notation as

$$|\psi\rangle = a\,|0\rangle + b\,|1\rangle \tag{54}$$

Where $|i\rangle$ is the 1s state localized at the i^{th} proton. In the $\{|0\rangle, |1\rangle\}$ basis our Hamiltonian can be written as

$$H = \begin{pmatrix}\langle 0|\hat{H}|0\rangle & \langle 1|\hat{H}|0\rangle \\ \langle 0|\hat{H}|1\rangle & \langle 1|\hat{H}|1\rangle\end{pmatrix} \equiv \begin{pmatrix}\epsilon & \Delta \\ \Delta & \epsilon\end{pmatrix} \tag{55}$$

Which is easily diagonalized to give the following eigenvector-eigenvalue pairs:

$$\psi_1 = \begin{pmatrix} 1 \\ 1 \end{pmatrix},\ E_1 = \epsilon + \Delta \text{ (Bonding)} \tag{56}$$

$$\psi_2 = \begin{pmatrix} 1 \\ -1 \end{pmatrix},\ E_2 = \epsilon - \Delta \text{ (Anti-bonding)} \tag{57}$$

It turns out that $\Delta < 0 \Leftrightarrow$ the bonding orbital is lower in energy (as seen in figure 6).

[1] W. M. C. Foulkes, L. Mitas, R. J. Needs, G. Rajagopal, Quantum monte carlo simulations of solids, Reviews of Modern Physics 73 (1).

[2] T. C. Scott, M. Aubert-Frecon, J. Grotendorst, New approach for the electronic energies of the hydrogen molecular ion, Chemical Physics 324, pp. 323-338.

[3] A. Kramida, Y. Ralchenko, J. Reader, NIST ASD Team, Nist atomic spectra database ionization energies data.

[4] W. Z. et al., Numerical solutions of the schrdinger equation for the ground lithium by the finite element method, Appl. Math. Comput. 153.

[5] E. Lindroth, H. Persson, S. Salomonson, A.-M. Mårtensson-Pendrill, Corrections to the beryllium ground-state energy, Physical review A 45 (3).

[6] E. R. Davidson, S. A. Hagstrom, S. J. Chakravorty, V. M. Umar, C. F. Fischer, Ground-state correlation energies for two- to ten-electron atomic ions, Physical Review A 44 (11).

[7] K. M. A. Kabir1, A. Halder, Estimation of boron ground state energy by monte carlo simulation, American Journal of Applied Mathematics 3 (3).

[8] C. Filippi, C. J. Huang, C. J. Umrigar, Spin contamination in quantum monte carlo wave functions, Chemical Physics 108 (21).